Environmental Pollution 364 (2025) 125325

Contents lists available at ScienceDirect

Environmental Pollution

journal homepage: www.elsevier.com/locate/envpol

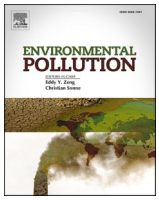

Potential source contribution function coupled with mass spectrometry detection to identify source of atmospheric polyethylene terephthalate☆

Hanling Yang [a], Junjie Zhang [b], Zhiwanxin Li [a], Jian Pu [c,d], Chu Peng [a], Chunguang Liu [a], Lei Wang [a,*]

[a] MOE Key Laboratory of Pollution Processes and Environmental Criteria/Tianjin Key Laboratory of Environmental Remediation and Pollution Control, College of Environmental Science and Engineering, Nankai University, Tianjin, 300350, China
[b] Department of Plant and Environmental Sciences (PLEN), University of Copenhagen, Thorvaldsensvej 40, DK-1871, Frederiksberg, Denmark
[c] Institute for the Advanced Study of Sustainability, United Nations University, Jingumae 5-53-70, Shibuya-ku, Tokyo, 150-8925, Japan
[d] Institute for Future Initiatives, The University of Tokyo, Tokyo, 113-0033, Japan

ARTICLE INFO

Keywords:
Atmospheric microplastics
Potential source contribution function
Polyethylene terephthalate
Liquid chromatography-tandem mass spectrometry

ABSTRACT

Source identification of atmospheric microplastics (MPs) is crucial for the development of mitigation policies. Compared with wind directions or backward trajectories of air masses, the potential source contribution function (PSCF) analysis identifies more comprehensive sources of atmospheric particles. However, conducting PSCF analysis requires hourly pollutant concentration data, which cannot be met by the atmospheric MPs abundance obtained through commonly used methods. In this study, total suspended particles (TSP) samples were collected hourly and the concentrations of atmospheric polyethylene terephthalate (PET) were detected using a liquid chromatography-tandem mass spectrometry. Atmospheric concentrations of PET MPs were 112.9 ± 39.04 ng/m^3 (average ± SD). Based on the hourly backward trajectories of air masses and the varied PET concentrations at the sampling site, potential sources of atmospheric PET were identified by PSCF analysis. The backward trajectory-based method indicates that atmospheric PET of the target site in this study primarily originates from dry farmlands. In comparison, both the residential areas and the dry farmlands were identified by PSCF as major sources of atmospheric PET at the receptor site. In contrast, both the backward-trajectory based method and PSCF analysis indicate that TSP mainly originates from the dry farmlands near the sampling site. This indicates that atmospheric PET in urban areas may have different sources from those of TSP, and PSCF is a suitable method for identifying sources of atmospheric PET.

1. Introduction

Microplastics (MPs) are plastic particles that are less than 5 mm in size, primarily originating from the degradation and fragmentation of larger plastic products or waste in the environment (Cole et al., 2011). Continuous environmental emissions and the non-degradable characteristics of plastic waste have resulted in the accumulation of MPs on Earth's surface (Brahney et al., 2021). Considering the potential hazards of MPs to both ecosystems and human health (Chen et al., 2024; Peng et al., 2021), the widespread presence of MPs has sparked increasing public concern. Due to their small size and low density, MPs can easily be carried into the atmosphere by air currents (Long et al., 2022). Given that there are no geographical boundaries in the atmospheric environment, MPs in the air can be transported (Chen et al., 2023; Wang et al., 2022) and serve as important sources for the input of MPs into terrestrial and aquatic environments (Zhang et al., 2020). The concentration of MPs in the atmosphere is highly correlated with population density (Liu et al., 2019); therefore, understanding the transport pathways and potential source distributions of atmospheric MPs in urban areas is essential for developing regulatory and mitigation strategies.

Wind direction can be used to identify the approximate direction of the source of atmospheric microplastics. However, it is too coarse to provide the distribution of potential sources of atmospheric particles (Szewc et al., 2020). Regions frequently traversed by air masses are more likely to be sources of air pollutants. Previous studies have already utilized the backward trajectory-based method to identify sources of

☆ This paper has been recommended for acceptance by Dr Michael Bank.

* Corresponding author.
E-mail address: wang2007@nankai.edu.cn (L. Wang).

https://doi.org/10.1016/j.envpol.2024.125325
Received 10 September 2024; Received in revised form 26 October 2024; Accepted 14 November 2024
Available online 16 November 2024

atmospheric MPs (Liu et al., 2025; Szewc et al., 2021). However, in areas with high emission concentrations but only a few air masses passing, the contribution of atmospheric pollution at the receptor site from these areas may be underestimated.

Potential Source Contribution Function (PSCF) is widely used to identify a comprehensive distribution of sources of atmospheric pollutants (Dos Santos and Hoinaski, 2021; Nogarotto et al., 2024). This method involves measuring the concentration of atmospheric pollutants at the receptor site as each air mass arrives. The calculation of the backward trajectories of air masses is usually performed at 1-h intervals (Wang et al., 2021). However, quantifying MPs by counting typically requires collecting atmospheric particulate samples for several hours, even using samplers with very high flow (1 m^3/min) (Wang et al., 2021; Yuan et al., 2023b). This limits the ability of PSCF in identifying the source locations of atmospheric MPs at the receptor site. Methods with high sensitivity, e.g. mass spectrometry, require a lower sample volume and a shorter sampling time, thereby enabling high-time-resolution observations of atmospheric MPs (Morioka et al., 2024). Therefore, by combining backward trajectories of air masses with the concentrations of atmospheric MPs detected by mass spectrometry, the PSCF analysis can be conducted to identify the sources of atmospheric MPs.

PET is a significant raw material for synthetic fibers (Peng et al., 2023), making it a representative type of MPs in urban atmospheric environments (Chang et al., 2023; Liu et al., 2019; Yuan et al., 2023b). Meanwhile, the mass spectrometry method we developed makes it possible to achieve quantitative detection of microplastic mass concentration using a small amount of environmental samples (Wang et al., 2017), and provides more precise results than manual counting and thereby reducing systematic errors (Zhang et al., 2020). Consequently, this provides the hourly atmospheric PET concentrations required for executing the PSCF model. In this study, atmospheric PET was detected using liquid-chromatography-tandem mass spectrometry. By integrating backward trajectories of air masses with concentrations of atmospheric PET, potential sources of atmospheric PET originating from various land cover types were identified by PSCF analysis. Moreover, total suspended particles (TSP) were also monitored during the same period, and the source distributions of TSP and atmospheric PET in urban areas were specifically compared.

2. Materials and method

2.1. Chemicals and materials

Standard PTA (Purified Terephthalic Acid, 99%) was purchased from Toronto Research chemicals, Inc (North York, ON, Canada). D_4-PTA (99%) was purchased from Sigma-Aldrich (St. Louis, MO, USA). HPLC-grade methanol was purchased from ANPEL Laboratory Technologies Inc. (Shanghai, China), and 1-pentanol was purchased from Meryer Chemical Technology Co., Ltd. (Shanghai, China). HLB (200 mg/6 mL) solid phase extraction cartridges (CNW, ANPEL Laboratory Technologies Inc., Shanghai, China) and Milli-Q water were also used in sample pretreatment and analysis.

2.2. Sample collection

From May 25 to June 10, 2024, TSP samples were collected hourly from 8:00 to 20:00 during the daytime hours using an active atmospheric particulate sampler (HVP-3300BRL/230, HI-Q, USA) with a flow rate of 1 m^3/min. The sampling site was located on an outdoor platform approximately 10 m above the ground level in the Jinnan district of Tianjin (117.34 E, 38.99 N) (Fig. 1). Jinnan district is one of Tianjin's suburban areas, and to its northwest are the densely populated six urban districts, which constitute the downtown area of Tianjin (Fig. 1 B). A total of 204 TSP samples were collected on pre-weighed glass fiber filter membranes (Whatman G/A) with a pore size of 0.2 μm. After sampling, the sampler was transferred to the laboratory, where the filter membrane was removed from the sampler using stainless steel tweezers. The filter membrane was dried at 60 °C in an oven, weighed, and subsequently wrapped in aluminum foil in preparation for the pretreatment required for mass spectrometry analysis.

2.3. Mass spectrometry analysis of PET polymers

The methods for mass spectrometry analysis of PET polymers have been published in previous studies (Wang et al., 2017; Zhang et al., 2021). The principle is that PET polymers are depolymerized into their monomer, PTA, after which the PTA background is removed, and the

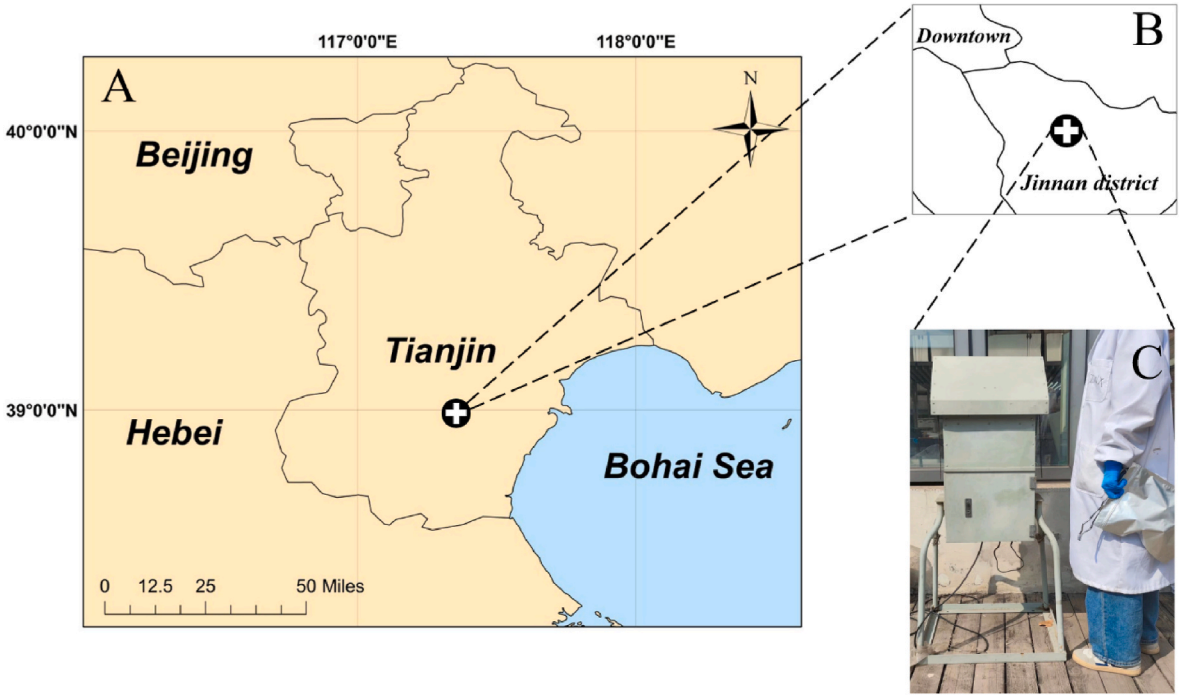

Fig. 1. Sampling location of atmospheric PET and TSP in Tianjin, China (A&B), and the 1 m^3/min active atmospheric particulate sampler used in this study (C).

PTA is analyzed by LC-MS/MS. The mass concentration' of PET polymers was calculated using this equation (Wang et al., 2017):

$$PTA_{amount} = \frac{PTA_{depolym} \times MW_{PTA-H_2O_2} / MW_{PTA}}{f_{(PTA-H_2O_2)}} \quad \text{(eq.1)}$$

where $PTA_{depolym}$ is the mass of PTA from the depolymerization of polymer, MW is the molecular weight, and $f_{(PTA-H_2O_2)}$ is mass percentage of PTA-H_2O_2 in PET plastics. PTA was analyzed by an Agilent 1260 system coupled with a triple quadrupole mass spectrometer (G6460C) (Agilent Technologies, Inc., Santa Clara, CA, USA). An Ultra AQ C_{18} column (100 mm × 2.1 mm, 3.0 μm, Restek Corporation, Bellefonte, PA, USA) was used for chromatographic separation of PTA. Details of the pretreatment of mass spectrometry analysis were shown in Text S1.

2.4. Backward trajectories and clustering

Lagrangian atmospheric models, such as the well-known Hybrid Single Particle Lagrangian Integrated Trajectory (HYSPLIT), are effective in identifying the origin of atmospheric pollutants by creating backward trajectories of air masses (Hee et al., 2023; Huang et al., 2021). The HYSPLIT model was developed by the National Oceanic and Atmospheric Administration (NOAA) of the United States, and has been used to demonstrate the transport of atmospheric MPs from urban to remote areas (Allen et al., 2019) and from the ocean to land (Liu et al., 2025; Szewc et al., 2021). In this study, the HYSPLIT model was operated in conjunction with the MeteoInfoMap 2.2.4 (China) (Wang, 2014). Meteorological data were obtained from the Global Data Assimilation System (GDAS). Backward trajectories of air masses arriving at the receptor site 10 m above the ground were calculated by HYSPLIT. The model was performed in backward mode for 1-h simulations, with 1-h time intervals. To observe the concentration of atmospheric PET when air masses reach the sampling point, each backward trajectory was calculated from the end time of sampling. Consequently, a total of 204 backward trajectories, covering the period from May 25 to June 10, 2024, between 9:00 and 20:00 daily, were calculated. The clustering of trajectories was conducted by MeteoinfoMap based on the Euclidean distance between trajectories (Wang, 2014).

Meteorological data of the sampling site, including pressure, temperature, relative humidity, wind speed and wind direction were obtained from the European Centre for Medium-Range Weather Forecasts (https://www.ecmwf.int/). Data of land cover types was obtained from China National Land Use/Cover Change (CNLUCC) (https://www.resdc.cn/).

2.5. Potential source contribution function

PSCF, a trajectory ensemble model, demonstrates the conditional probability that an air pollutant with concentrations above a given criterion arrives at a receptor site after traveling at a certain height above the ground (Nogarotto et al., 2024). By combining backward trajectories of air masses with time-resolved concentrations of atmospheric pollutants observed at the receptor site, the likely locations of emission sources contributing to pollutant concentrations higher than a specific criterion at the receptor site can be identified by PSCF (Dos Santos and Hoinaski, 2021).

When an air mass reaches the receptor site, the concentration of air pollutants at the receptor site should be observed simultaneously. If the concentration of an air pollutant at the receptor site exceeds the set criterion when an air mass arrives, then the areas through which the backward trajectory of the air mass passed are likely sources of the air pollutant. In this study, a grid that covering the backward trajectories originating from the receptor site was created using MeteoInfoMap. The PSCF value for the *ij*-th grid cell can be calculated according to equation (2) (Liu et al., 2013),

$$PSCF_{ij} = m_{ij} / n_{ij} \quad \text{(eq.2)}$$

where m_{ij} represents the number of trajectory endpoints that ending or crossing the *ij*-th grid cell that correspond to pollutant concentrations above a set criterion (that is, the average concentration of atmospheric PET observed at the sampling site), and n_{ij} represents the total number of trajectory endpoints in the same grid cell.

2.6. Quality control and quality assurance

Glass vessels and stainless steel tweezers were rinsed twice with Milli-Q water before use. Glass fiber filter membranes and rinsed glass vessels were wrapped in aluminum foil and baked at 500 °C in a muffle furnace for 4 h before use (Liu et al., 2019). The processes of removing the filter membrane from the sampler, weighing it, and pretreating it for mass spectrometry analysis were all carried out in a fume hood. Plastic products were avoided except for PP tubes and pipette tips. Process blanks through the entire pretreatment were conducted. Each filter was cut into three equal-sized pieces, and the average of the mass spectrometry detections from the three pieces was used as the final concentration for the sample. The procedure blank was analyzed after every set of 12 samples during mass spectrometry detection, with the average concentration of 2.7 ± 0.3 ng/m^3. During mass spectrometry detection, a calibration standard was injected after every set of 12 samples to check the instrumental drift in sensitivity, and a pure solvent was injected to check the carry-over of target chemicals from sample to sample during the detection process.

2.7. Statistical analysis

Pearson's correlation and *t*-test were conducted using SPSS 25 (IBM, NY, U.S.A.). Significance was considered when $p < 0.05$. The box plot, correlation plot and pollutant rose diagrams were generated using Origin 2024b software (OriginLab Corporation, MA, U.S.A). Land cover types near the receptor site was generated in ArcMap 10.2 software (ESRI, U.S.A).

3. Results and discussion

3.1. Concentrations of atmospheric PET and TSP in Tianjin

In this study, atmospheric PET was collected hourly from May 25 to June 11, 2024, during daytime hours. The concentration of atmospheric PET was 112.9 ± 39.04 ng/m^3 (Fig. 2A). In East Asia, atmospheric PET concentrations of 227 ng/m^3 have been reported in the urban areas (Morioka et al., 2024), which is similar to the concentration detected in this study. Meteorological factors, including wind speed, wind direction, relative humidity, pressure, and temperature may influence the concentrations of particulate matter in the atmosphere (Wang et al., 2021; Yuan et al., 2023b). In this study, significantly higher concentrations of atmospheric PET ($p < 0.05$) were found when northwest winds prevailed (Fig. 2C). Winds can facilitate the transport of MPs in the atmosphere, leading to the variation of atmospheric MPs concentrations (Allen et al., 2019; Liu et al., 2025; Szewc et al., 2021). The direction to the northwest of the sampling site is near the downtown area of Tianjin (Fig. 1B), which is densely populated. Thus, higher concentrations of PET over downtown may be transported to downwind regions by the wind. A similar MPs distribution was also found in our previous study of dust-fall samples in Tianjin, where the PET concentration was significantly higher in the downtown area (Zhang et al., 2021).

During the same period, the concentration of TSP was 290.0 ± 69.60 μg/m^3 (Fig. 2A). A significant negative correlation was observed between the concentration of TSP and relative humidity ($p < 0.001$, Fig. 2B). Suspended particles, such as black carbon and mineral dust, absorb water in the atmosphere (Liu et al., 2021; Su et al., 2024), which

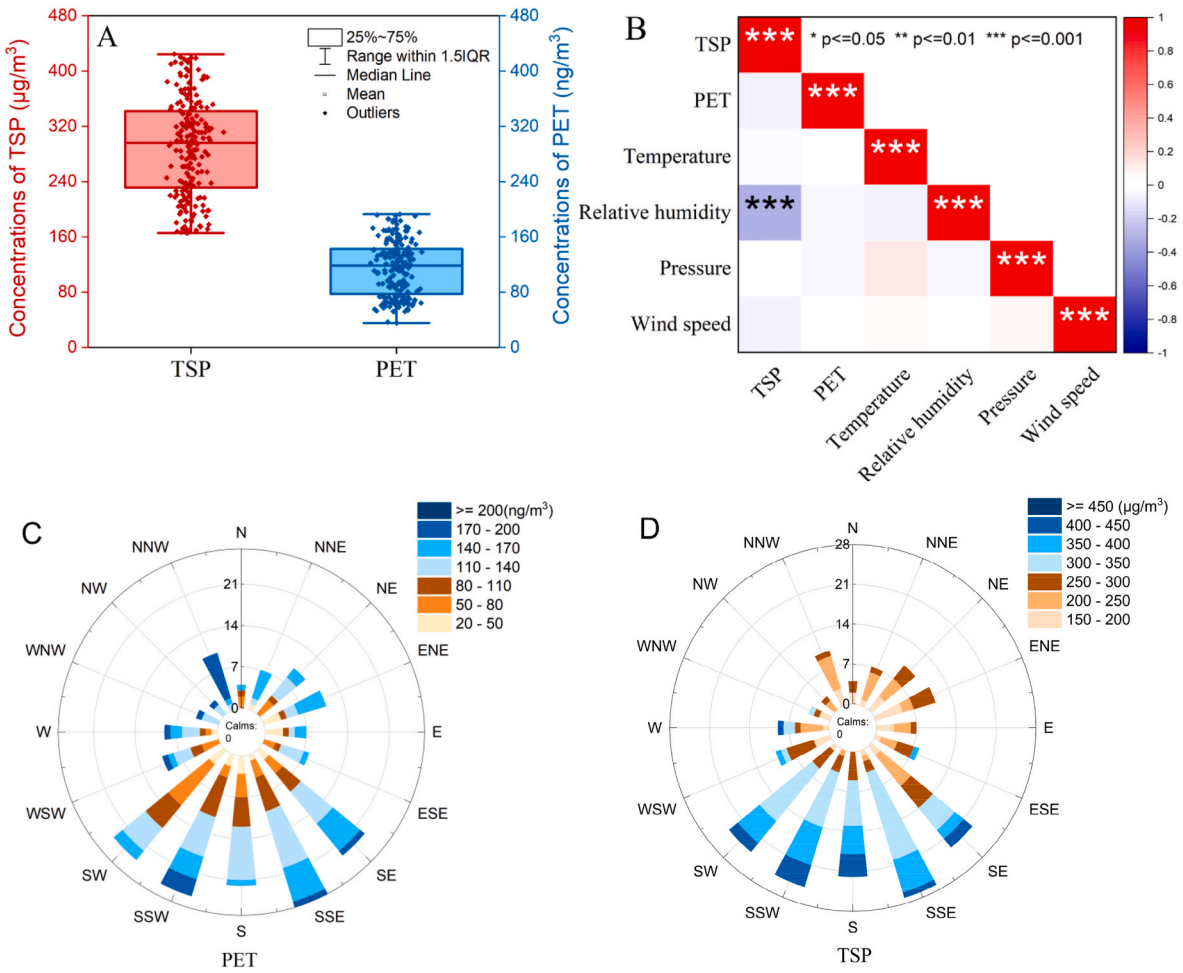

Fig. 2. Concentrations of atmospheric PET and TSP (A), correlations between concentrations of atmospheric PET, TSP and meteorological factors (B), and the pollutant rose maps of atmospheric PET (C) and TSP (D).

increases their density and accelerating their settling (Yuan et al., 2023a). In comparison, PET has relatively poor hygroscopicity(Liu et al., 2020), suggesting it may be less influenced by changes in relative humidity compared to TSP. The concentrations of TSP were significantly higher under the south-southwest (SSW) and south-southeast (SSE) wind directions ($p < 0.05$ Fig. 2D). Due to the dry and windy climate in northern China, soil fugitive dust has become one of the most important sources of TSP pollution (Li et al., 2018). Building density is low in the area south of the sampling site. In open environments, the wind is commonly stronger, which facilitates the lifting of soil dust from the ground into the air (Pi et al., 2019). High atmospheric PET concentrations downwind of densely populated areas, along with high TSP concentrations downwind of barren soil, result in the weak correlation ($p > 0.05$, Fig. 2B) observed between atmospheric PET and TSP concentrations at the sampling site.

3.2. *Integrated modeling to identify potential sources of atmospheric PET*

Backward trajectories of air masses, calculated by the HYSPLIT model, have been widely used to identify source locations of atmospheric particles including MPs (Ankit et al., 2024; Liu et al., 2025; Wang et al., 2021). Theoretically, regions frequently passed by backward trajectories are more likely to be identified as air pollution sources (Allen et al., 2019). However, even in areas less frequently passed by backward trajectories, significant source emissions in these areas may still affect the atmospheric pollutant load at the receptor site. In the present study, backward trajectories of air masses arriving at the receptor site were calculated by the HYSPLIT model, which was performed in backward mode for 1-h simulations, with 1-h time intervals. A total of 204 backward trajectories of air masses were calculated and then clustered into eight primary pathways using MeteoinfoMap (Fig. 3). The clusters of backward trajectories for the sampling site were mainly located between the southwest and southeast directions (Fig. 3). However, the highest concentrations of atmospheric PET were observed under the northwest wind direction (Fig. 2C), which was the direction with the lowest frequency of backward trajectories (3.92%, Fig. 3). This indicates that neither wind directions nor the backward trajectory-based method can fully reflect the comprehensive distribution of source locations of atmospheric PET.

To further identify probable locations of emission sources that affect atmospheric PET load at the sampling site, the potential source contribution function (PSCF) analysis was conducted (Fig. 4A and B). PSCF analysis combines the concentrations of atmospheric pollutants and backward trajectories of air masses (Nogarotto et al., 2024). In brief, researching areas are divided into grids of cells (0.05° × 0.05°), the higher the PSCF values in a grid cell, the more likely it is to be the source location of atmospheric PET at the receptor site. For atmospheric PET at the sampling site, source locations identified by the wind directions (Fig. 2C) and the backward trajectory-based method (Fig. 3) were different. Only the PSCF analysis showed a comprehensive distribution of atmospheric PET sources (Fig. 4A), indicating that both the residential areas to the northwest of the sampling site, as well as the dry farmland to the south of the sampling site (Fig. 4A and C), are important sources of atmospheric PET.

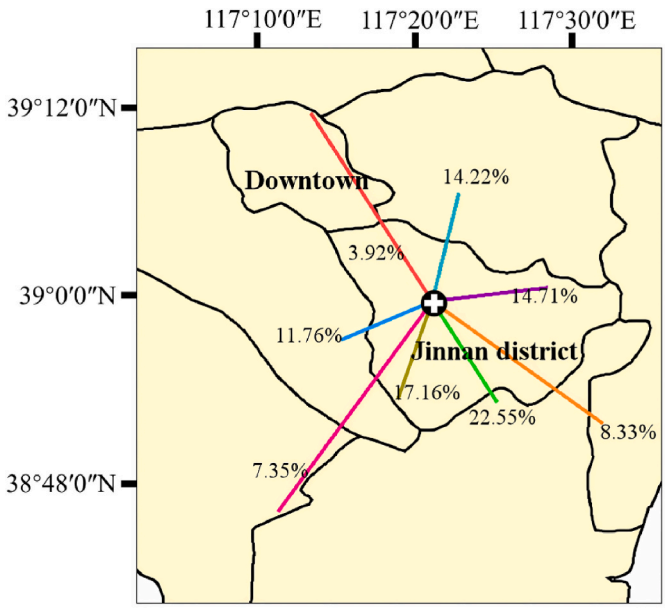

Fig. 3. Clusters of backward trajectories of air masses arriving at the receptor site (represented by the white cross).

3.3. Potential sources identification of atmospheric PET and TSP

Areas with high PSCF values (>0.6) for atmospheric PET were primarily distributed in three directions, including the northwest, north-northeast and south of the receptor site (Fig. 4A), indicating that the sources of atmospheric PET were mainly scattered in these regions. The northwest of the receptor site showed PSCF values exceeding 0.8 (Fig. 4A), indicating this area as the most likely source for atmospheric PET at the receptor site. This aligns with the source location identified by wind directions, suggesting the northwest as a significant source of atmospheric PET (Fig. 2C). The source location to the north-northeast of the sampling site was not identified by the wind directions. Although 14.22% backward trajectories originated from this direction, atmospheric PET was considered to originate more from the south-southwest and south-southeast of the sampling site, with 17.16% and 22.55% of the backward trajectories found in these two directions (Fig. 3). However, higher PSCF values (>0.8) were observed in the north-northeast of the sampling site (Fig. 4A). This is because PSCF can identify areas that, despite being passed by a lower frequency of backward trajectories, emit relatively higher concentrations of pollutants. Land cover types around the sampling site were analyzed, with both the northwest and north-northeast of the sampling site being urban residential areas (Fig. 4C). A number of textiles are present in residential areas, and the shedding of plastic fibers from these materials can result in the release of textile MPs into the environment (Peng et al., 2023). For instance, washing a blanket once a week will contribute to as many as 3×10^3 fibers released (O'Brien et al., 2020). The textile MPs may enter the atmosphere due to indoor-outdoor air convection and improper management (Shi et al., 2023), resulting in higher PET concentrations in the air of residential areas than in other ecosystems (Zhang et al., 2023). Despite the lower frequency of trajectories passing through the northwest and north-northeast of the sampling site (Fig. 3), these two areas, with their higher atmospheric PET concentrations, may still significantly affect the atmospheric PET load at the receptor site. The southern region of the receptor site (mainly near the boundary of Jinnan district) also exhibited high PSCF values for atmospheric PET (Fig. 4A), with the predominant land cover type being dry farmland (Fig. 4C). Dry farmland refers to agricultural fields that rely primarily on natural rainfall for crop cultivation. When there are no crops on the surface of dry farmland, wind can lead to the emission of soil particles into the atmosphere (Zhang et al., 2023). In Tianjin, the main crops, soybeans and corn, are typically sown in May. Thus, the lack of vegetation on the surface of corn and soybean fields makes it easy for the ground soil particles to be lifted by wind into the air during the sampling period. Therefore, the dry farmland can still become an important source for atmospheric PET when trajectories of air masses frequently pass over it (Fig. 3), although the atmospheric PET concentration of dry farmland may be lower than that of residential areas (Zhang et al., 2023).

The source location of TSP at the sampling site was also identified by PSCF, based on equation (2), where m_{ij} represents the number of trajectory endpoints that end or cross the *ij*-th grid cell that corresponds to TSP concentrations above the average values observed at the sampling site. High PSCF values of TSP were mainly observed near the boundary of Jinnan district, to the south of the receptor site (Fig. 4B), suggesting that the south of the sampling site is a significant emission source of TSP at the sampling site. This corresponds to the source location of TSP identified by wind directions (Fig. 2D) and backward trajectories (Fig. 3). Particles released from dry farmland to the south of the sampling site (Fig. 4C) are likely to be a major source of TSP. This result is similar to the source distribution of TSP in urban areas of India, which also indicates that TSP significantly originates from dry lands through which air masses pass (Raman and Ramachandran, 2011).

For TSP at the sampling site, source locations identified by the wind directions (Fig. 2D), the backward trajectory-based method (Fig. 3) and the PSCF analysis (Fig. 4B) were the same. However, the sources of atmospheric MPs are usually complex (Parashar and Hait, 2023). Therefore, in urban areas with significant sources of atmospheric PET, such as residential areas, it is not advisable to rely solely on wind directions or backward trajectories to identify the source locations of atmospheric PET. PSCF analysis can map out the source locations of atmospheric particles at the receptor site comprehensively. However, conducting the PSCF analysis commonly requires atmospheric pollutant concentration data with hourly time resolution, which is not achievable using the MPs quantification method that relies on counting (Yuan et al., 2023b). In contrast, a sensitive mass spectrometry method is able to quantify PET even with a small number of samples (Zhang et al., 2021), thus providing the concentration data needed for PSCF analysis.

4. Conclusion

The atmospheric PET concentration detected by mass spectrometry can meet the requirements of the PSCF model. Using the method of mass concentration based PSCF, the source location of atmospheric PET can be determined. PSCF analysis in this study indicates that TSP at the target site is mainly originates from dry farmlands, whereas PET MPs originates from both residential areas and dry farmlands, which illustrates atmospheric MPs have more complex sources than TSP in urban areas. Compared to the backward trajectory-based method, which suggests that atmospheric PET primarily originates from dry farmlands, the PSCF analysis demonstrates a more comprehensive source map of atmospheric PET. This indicates that the combined approach of mass spectrometry detection and PSCF calculation is very helpful for identifying potential sources of atmospheric MPs, which are typically complex in urban environments.

CRediT authorship contribution statement

Hanling Yang: Writing – original draft, Visualization, Investigation, Formal analysis, Data curation, Conceptualization. **Junjie Zhang:** Validation, Methodology. **Zhiwanxin Li:** Investigation. **Jian Pu:** Validation. **Chu Peng:** Formal analysis. **Chunguang Liu:** Supervision. **Lei Wang:** Writing – original draft, Project administration, Funding acquisition, Conceptualization.

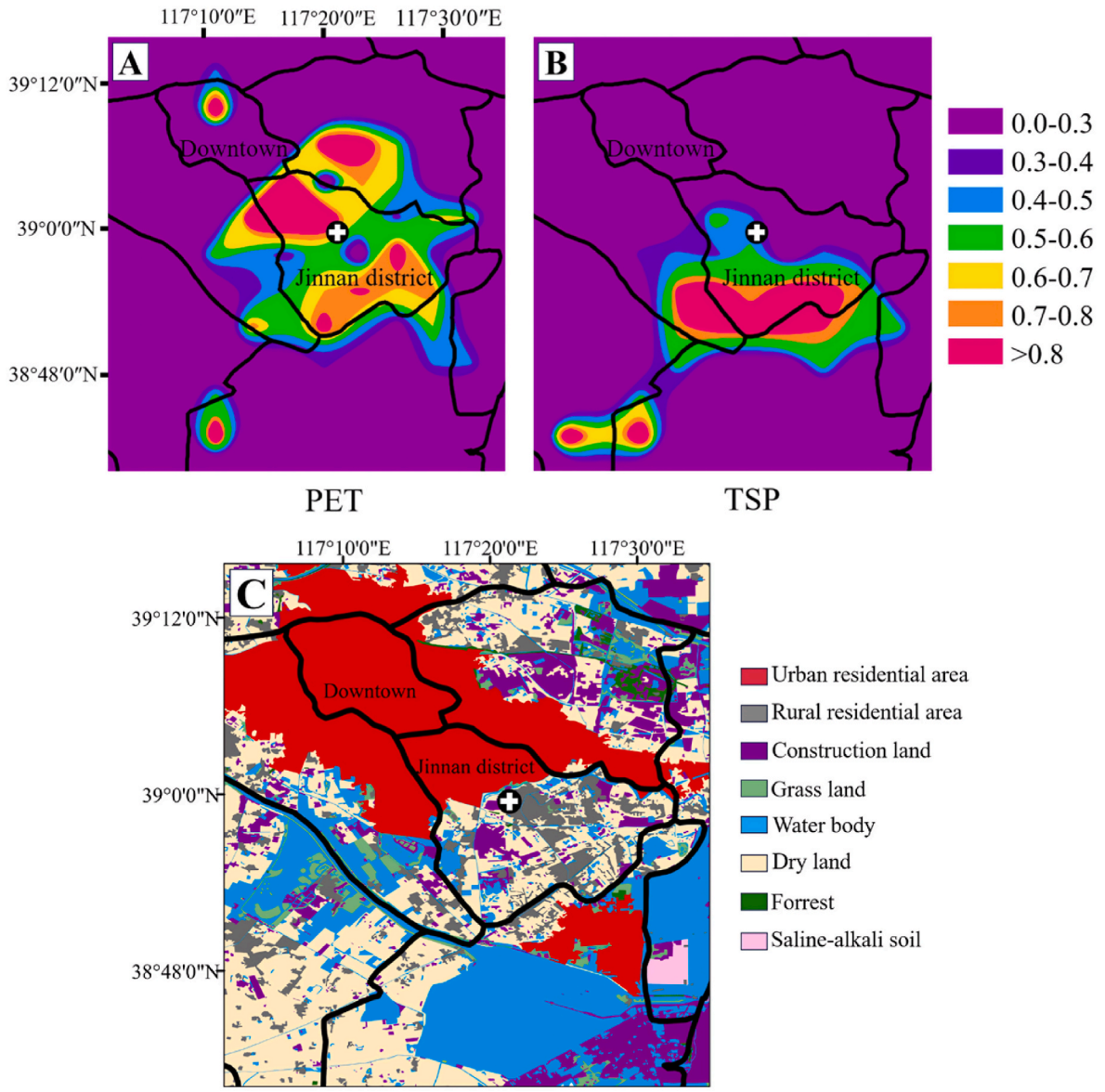

Fig. 4. PSCF distribution maps of atmospheric PET (A) and TSP (B) at the receptor site, with the white across representing the location of sampling site, and the legend depicting the range of PSCF values. The land cover types around the receptor site (C).

Declaration of competing interest

The authors declare that they have no known competing financial interests or personal relationships that could have appeared to influence the work reported in this paper.

Acknowledgement

This work was supported by the National Natural Science Foundation of China (42077336 & 42177373), the Asia-Pacific Network for Global Change Research (CRRP2019-FP06-WANG), the 111 Program of the Ministry of Education, China (T2017002), and the Fundamental Research Funds for the Central Universities of China. We appreciate the advice supported by Dr. Yingze Tian at Nankai University and Dr. Pengfei Wu at Nanjing Forestry University.

Appendix A. Supplementary data

Supplementary data to this article can be found online at https://doi.org/10.1016/j.envpol.2024.125325.

Data availability

Data will be made available on request.

References

Allen, S., Allen, D., Phoenix, V.R., Le Roux, G., Durántez Jiménez, P., Simonneau, A., Binet, S., Galop, D., 2019. Atmospheric transport and deposition of microplastics in a remote mountain catchment. Nat. Geosci. 12 (5), 339–344. https://doi.org/10.1038/s41561-019-0335-5.

Ankit, Y., Ajay, K., Nischal, S., Kaushal, S., Kataria, V., Dietze, E., Anoop, A., 2024. Atmospheric deposition of microplastics in an urban conglomerate near to the foothills of Indian Himalayas: investigating the quantity, chemical character, possible sources and transport mechanisms. Environ. Pollut. 124629. https://doi.org/10.1016/j.envpol.2024.124629.

Brahney, J., Mahowald, N., Prank, M., Cornwell, G., Klimont, Z., Matsui, H., Prather, K. A., 2021. Constraining the atmospheric limb of the plastic cycle. Proc. Natl. Acad. Sci. USA 118 (16), e2020719118. https://doi.org/10.1073/pnas.2020719118.

Chang, D.Y., Jeong, S., Shin, J., Park, J., Park, C.R., Choi, S., Chun, C.H., Chae, M.Y., Lim, B.C., 2023. First quantification and chemical characterization of atmospheric microplastics observed in Seoul, South Korea. Environ. Pollut. 327, 121481. https://doi.org/10.1016/j.envpol.2023.121481.

Chen, Q., Shi, G., Revell, L.E., Zhang, J., Zuo, C., Wang, D., Le Ru, E.C., Wu, G., Mitrano, D.M., 2023. Long-range atmospheric transport of microplastics across the

southern hemisphere. Nat. Commun. 14 (1), 7898. https://doi.org/10.1038/s41467-023-43695-0.
Chen, Y., Meng, Y., Liu, G., Huang, X., Chai, G., Xie, Y., 2024. Atmospheric deposition of microplastics at a western China metropolis: relationship with underlying surface types and human exposure. Environ. Pollut. 355, 124192. https://doi.org/10.1016/j.envpol.2024.124192.
Cole, M., Lindeque, P., Halsband, C., Galloway, T.S., 2011. Microplastics as contaminants in the marine environment: a review. Mar. Pollut. Bull. 62, 2588–2597. https://doi.org/10.1016/j.marpolbul.2011.09.025.
Dos Santos, O.N., Hoinaski, L., 2021. Incorporating gridded concentration data in air pollution back trajectories analysis for source identification. Atmos. Res. 263, 105820. https://doi.org/10.1016/j.atmosres.2021.105820.
Hee, Y.Y., Hanif, N.M., Weston, K., Latif, M.T., Suratman, S., Rusli, M.U., Mayes, A.G., 2023. Atmospheric microplastic transport and deposition to urban and pristine tropical locations in Southeast Asia. Sci. Total Environ. 902, 166153. https://doi.org/10.1016/j.scitotenv.2023.166153.
Huang, Y., He, T., Yan, M., Yang, L., Gong, H., Wang, W., Qing, X., Wang, J., 2021. Atmospheric transport and deposition of microplastics in a subtropical urban environment. J. Hazard Mater. 416, 126168. https://doi.org/10.1016/j.jhazmat.2021.126168.
Li, T., Bi, X., Dai, Q., Liu, B., Han, Y., You, H., Wang, L., Zhang, J., Cheng, Y., Zhang, Y., Wu, J., Tian, Y., Feng, Y., 2018. Improving spatial resolution of soil fugitive dust emission inventory using RS-GIS technology: an application case in Tianjin, China. Atmos. Environ. 191, 46–54. https://doi.org/10.1016/j.atmosenv.2018.07.051.
Liu, J.J., Wang, W., Yu, D., Zhao, K., 2020. Durable moisture-wicking and fast-dry polyester fabric prepared by UV-induced click reaction. Fibers Polym. 21, 111–118. https://doi.org/10.1007/s12221-020-9466-y.
Liu, P.J., Shao, L.Y., Guo, Z.Y., Zhang, Y.X., Cao, Y.X., Ma, X.Y., Morawska, L., 2025. Physicochemical characteristics of airborne microplastics of a typical coastal city in the Yangtze River Delta Region, China. J. Environ. Sci. 148, 602–613. https://doi.org/10.1016/j.jes.2023.09.027.
Liu, K., Wang, X., Fang, T., Xu, P., Zhu, L., Li, D., 2019. Source and potential risk assessment of suspended atmospheric microplastics in Shanghai. Sci. Total Environ. 675, 462–471. https://doi.org/10.1016/j.scitotenv.2019.04.110.
Liu, N., Yu, Y., He, J., Zhao, S., 2013. Integrated modeling of urban–scale pollutant transport: application in a semi-arid urban valley, Northwestern China. Atmos. Pollut. Res. 4 (3), 306–314. https://doi.org/10.5094/APR.2013.034.
Liu, W.Y., Li, J., Gu, W.J., Santos, L.F., Boman, J., Zhang, X., Tang, M., Wang, S., Kong, X., 2021. Chemical and hygroscopic characterization of surface salts in the qaidam basin: implications for climate impacts on planet Earth and mars. ACS Earth Space Chem. 5 (3), 651–662. https://doi.org/10.1021/acsearthspacechem.0c00339.
Long, X., Fu, T.M., Yang, X., Tang, Y., Zheng, Y., Zhu, L., Shen, H., Ye, J., Wang, C., Wang, T., Li, B., 2022. Efficient atmospheric transport of microplastics over Asia and adjacent oceans. Environ. Sci. Technol. 56 (10), 6243–6252. https://doi.org/10.1021/acs.est.1c07825.
Morioka, T., Tanaka, S., Kohama-Inoue, A., Watanabe, A., 2024. The quantification of the airborne plastic particles of 0.43–11 μm: procedure development and application to atmospheric environment. Chemosphere 351, 141131. https://doi.org/10.1016/j.chemosphere.2024.141131.
Nogarotto, D.C., Gimbernau, J., Pozza, S.A., 2024. PSCF method for source identification of particulate matter in an agricultural background region in Brazil. Environ. Technol. https://doi.org/10.1080/09593330.2024.2334292.
O'Brien, S., Okoffo, E.D., O'Brien, J.W., Ribeiro, F., Wang, X., Wright, S.L., Samanipour, S., Rauert, C., Toapanta, T.Y.A., Albarracin, R., Thomas, K.V., 2020. Airborne emissions of microplastic fibres from domestic laundry dryers. Sci. Total Environ. 747, 141175. https://doi.org/10.1016/j.scitotenv.2020.141175.
Parashar, N., Hait, S., 2023. Plastic rain—atmospheric microplastics deposition in urban and peri-urban areas of Patna City, Bihar, India: distribution, characteristics, transport, and source analysis. J. Hazard Mater. 458, 131883. https://doi.org/10.1016/j.jhazmat.2023.131883.
Peng, C., Zhang, X., Li, M., Lu, Y., Liu, C., Wang, L., 2023. Source apportionment of microplastics in indoor dust: two strategies based on shape and composition. Environ. Pollut. 334, 122178. https://doi.org/10.1016/j.envpol.2023.122178.
Peng, C., Zhang, X.F., Zhang, X., Liu, C.G., Chen, Z., Sun, H.W., Wang, L., 2021. Bacterial community under the influence of microplastics in indoor environment and the health hazards associated with antibiotic resistance genes. Environ. Sci. Technol. 56 (1), 422–432. https://doi.org/10.1021/acs.est.1c04520.
Pi, H.W., Sharratt, B., Lei, J.Q., 2019. Wind erosion and dust emissions in central Asia: spatiotemporal simulations in a typical dust year. Earth Surf. Process. Landforms 44, 521–534. https://doi.org/10.1002/esp.4514.
Raman, R.S., Ramachandran, S., 2011. Source apportionment of the ionic components in precipitation over an urban region in Western India. Environ. Sci. Pollut. Res. 18, 212–225. https://doi.org/10.1007/s11356-010-0365-4.
Shi, Y.F., Chai, J.Q., Xu, T., Ding, L.H., Huang, M.J., Gan, F.M., Pi, K.W., Gerson, A.R., Yang, J.K., 2023. Microplastics contamination associated with low-value domestic source organic solid waste: a review. Sci. Total Environ. 857, 159679. https://doi.org/10.1016/j.scitotenv.2022.159679.
Su, Z.Y., Chen, L.X.D., Liu, Y., Zhang, P., Chen, T.Z., Chu, B.W., Tang, M.J., Ma, Q.X., He, H., 2024. A study on the influence of inorganic ions, organic carbon and microstructure on the hygroscopic property of soot. Atmos. Chem. Phys. 24 (2), 993–1003. https://doi.org/10.5194/acp-24-993-2024.
Szewc, K., Graca, B., Dołęga, A., 2021. Atmospheric deposition of microplastics in the coastal zone: characteristics and relationship with meteorological factors. Sci. Total Environ. 761, 143272. https://doi.org/10.1016/j.scitotenv.2020.143272.
Wang, L., Zhang, J.J., Hou, S.G., Sun, H.W., 2017. A simple method for quantifying polycarbonate and polyethylene terephthalate microplastics in environmental samples by liquid chromatography–tandem mass spectrometry. Environ. Sci. Technol. Lett. 4 (12), 530–534. https://doi.org/10.1021/acs.estlett.7b00454.
Wang, X., Liu, K., Zhu, L., Li, C., Song, Z., Li, D., 2021. Efficient transport of atmospheric microplastics onto the continent via the East Asian summer monsoon. J. Hazard Mater. 414, 125477. https://doi.org/10.1016/j.jhazmat.2021.125477.
Wang, Y.Q., 2014. MeteoInfo: GIS software for meteorological data visualization and analysis. Meteorol. Appl. 21 (2), 360–368. https://doi.org/10.1002/met.1345.
Wang, Z., Zhang, Y., Kang, S., Yang, L., Luo, X., Chen, P., Guo, J., Hu, Z., Yang, C., Yang, Z., Gao, T., 2022. Long-range transport of atmospheric microplastics deposited onto glacier in southeast Tibetan Plateau. Environ. Pollut. 306, 119415. https://doi.org/10.1016/j.envpol.2022.119415.
Yuan, Y., Li, S., Chen, T., Ren, J., 2023. Effects of ambient temperature and humidity on natural deposition characteristics of airborne biomass particles. Int. J. Environ. Res. Publ. Health 20 (3), 1890. https://doi.org/10.3390/ijerph20031890.
Yuan, Z., Pei, C., Li, H., Lin, L., Liu, S., Hou, R., Liao, R., Xu, X., 2023. Atmospheric microplastics at a southern China metropolis: occurrence, deposition flux, exposure risk and washout effect of rainfall. Sci. Total Environ. 869, 161839. https://doi.org/10.1016/j.scitotenv.2023.161839.
Zhang, R., Jia, X., Wang, K., Lu, L., Li, F., Li, J., Xu, L., 2023. Characteristics, sources and influencing factors of atmospheric deposition of microplastics in three different ecosystems of Beijing. China. Sci. Total Environ. 883, 163567. https://doi.org/10.1016/j.scitotenv.2023.163567.
Zhang, Y., Kang, S., Allen, S., Allen, D., Gao, T., Sillanpää, M., 2020. Atmospheric microplastics: a review on current status and perspectives. Earth Sci. Rev. 203, 103118. https://doi.org/10.1016/j.earscirev.2020.103118.
Zhang, Y., Peng, Y., Peng, C., Wang, P., Lu, Y., He, X., Wang, L., 2021. Comparison of detection methods of microplastics in landfill mineralized refuse and selection of degradation degree indexes. Environ. Sci. Technol. 55 (20), 13802–13811. https://doi.org/10.1021/acs.est.1c02772.